ADVANCES IN PHYSICS: X, 2016
VOL. 1, NO. 4, 523–543
http://dx.doi.org/10.1080/23746149.2016.1221739

Taylor & Francis
Taylor & Francis Group

REVIEW ARTICLE

OPEN ACCESS

Optical methods for quantitative and label-free sensing in living human tissues: principles, techniques, and applications

Robert H. Wilson[a], Karthik Vishwanath[b] and Mary-Ann Mycek[c]

[a]Beckman Laser Institute, University of California, Irvine, CA, USA; [b]Department of Physics, Miami University, Oxford, OH, USA; [c]Department of Biomedical Engineering, Applied Physics Program, University of Michigan, Ann Arbor, MI, USA

ABSTRACT

We present an overview of quantitative and label-free optical methods used to characterize living biological tissues, with an emphasis on emerging applications in clinical tissue diagnostics. Specifically, this review focuses on diffuse optical spectroscopy, imaging, and tomography, optical coherence-based techniques, and nonlinear optical methods for molecular imaging. The potential for non- or minimally invasive assessment, quantitative diagnostics, and continuous monitoring enabled by these tissue-optics technologies provides significant promise for continued clinical translation.

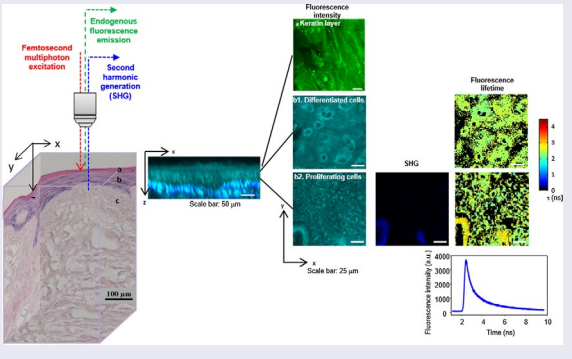

ARTICLE HISTORY
Received 10 May 2016
Accepted 27 July 2016

KEYWORDS
Tissue optics; diffuse optical spectroscopy; laser speckle imaging; diffuse correlation spectroscopy; multi-photon microscopy; second-harmonic generation; coherent anti-stokes Raman

PACS
87.57 (Medical imaging); 87.64 (Spectroscopic and microscopic techniques in biophysics and medical physics); 42.62.Be (Laser applications: Biological and medical applications); 42.30.Wb (Image reconstruction; tomography)

1. Introduction

Measuring the interaction of light with biological tissues can tell us about tissue morphology and biological function on the microscopic, mesoscopic, and macroscopic levels. Light–tissue interactions have been known for millennia, but over the past century (and particularly since the invention of the laser), researchers have developed a number of clinically compatible techniques in which light with

CONTACT Robert H. Wilson wilsonrh@uci.edu

Table 1. Overview of tissue-optics methods discussed in this review, including diffuse optical spectroscopy and tomography (DOS/DOT), laser speckle contrast imaging and diffuse correlation spectroscopy (LSCI/DCS), and nonlinear optical (NLO) molecular sensing methods.

Technique	Physical process	Light source and spectral range	Origin of contrast within tissue	Quantitative endpoints
DOS/DOT	Diffuse photon waves	Broadband lamp or set of LEDs; typically visible to near-infrared	Absorption and scattering	Hemoglobin concentration and oxygenation; Scatterer concentration and morphology
LSCI/DCS	Coherent waves	Laser; typically near-infrared	Particle motion	Changes in blood flow velocity
Nonlinear Optical (NLO) Molecular Imaging	Two-Photon Excitation Fluorescence (TPEF)	Pulsed laser; typically far visible to near-infrared	Molecular absorption	Fluorophore concentration and spatial distribution; Fluorophore binding with microenvironment (using FLIM)
	Second-Harmonic Generation (SHG)	Pulsed laser; typically far visible to near-infrared	Non-centrosymmetric structures	Concentration, spatial distribution, and orientation

prescribed properties (e.g. wavelength, frequency, coherence, spatial profile) is shone onto tissue, and the portion of this light that returns to the surface is detected as a function of these same variables. Interaction with the tissue perturbs the light in a manner that can be detected and quantified by optical instrumentation coupled with mathematical light transport models. This information can be employed to assess the health of tissue and characterize its response to perturbation.

One advantage of these methods is that they frequently interrogate endogenous optical contrast in tissues from, e.g. absorbing, scattering, or fluorescing tissue constituents. Therefore, many of these methods do not require an exogenous contrast agent (such as a fluorescent dye) to probe tissue structure and function. Another objective advantage of these techniques is that they are quantitative (to a first approximation), using light–tissue interaction models to extract perturbation-induced changes in concentrations of absorbers (e.g. hemoglobin, water, lipid), scatterers (e.g. collagen, cells, organelles), and fluorophores (e.g. collagen, NADH, FAD) within the tissue. For instance, these techniques can include hybrid photon-wave descriptions of diffuse light (Section 2), coherence- and interference-based effects (Sections 3 and 4), or modeled in terms of photon absorption and scattering (Section 4). These techniques span multiple spatial and temporal scales and have reached various points along the path toward clinical and/or commercial translation.

In this review, we will discuss three widely used methods in tissue optics (Table 1): diffuse optical techniques (Section 2), coherence-based techniques (Section 3), and nonlinear optical techniques (Section 4).

2. Diffuse optical spectroscopy (DOS), imaging, and tomography

2.1. Diffuse optical spectroscopy

DOS techniques have been employed for over two decades to quantitatively characterize biological tissues in pre-clinical and clinical settings [1–7]. DOS methods

typically interrogate endogenous contrast from absorption and scattering of light by tissue. Tissue components such as water, lipid, and oxygenated and deoxygenated hemoglobin (HbO2, Hb) have distinct light absorption profiles in the visible, near-infrared, and short-wave infrared regions of the electromagnetic spectrum [6]. The optical absorption coefficient $\mu_a(\lambda)$ of the tissue can be represented as a linear combination of the extinction coefficients $\varepsilon_i(\lambda)$ of these chromophores, weighted by their concentrations c_i within the tissue: $\mu_a(\lambda) = \Sigma c_i \varepsilon_i(\lambda)$ [4]. For light that has undergone enough scattering events to be considered diffuse, the optical scattering coefficient $\mu_s(\lambda)$ of the tissue can be modeled with a power law of the form $\mu_s(\lambda) = A(\lambda/\lambda_0)^{-b}$, where A and b are referred to as the scattering amplitude and power, respectively, and λ_0 is an arbitrary reference wavelength. In diffuse regimes, the scattering of the tissue is typically represented with the reduced scattering coefficient $\mu_s'(\lambda) = \mu_s(\lambda)(1-g(\lambda))$, which is a combination of the scattering coefficient $\mu_s(\lambda)$ and the scattering anisotropy $g(\lambda)$ (defined as the mean cosine of the scattering angle) [7].

The tissue absorption and scattering properties are obtained by illuminating the tissue with broadband light (e.g. using a tungsten–halogen lamp) or light at several discrete wavelength bands (e.g. using light-emitting diodes) and detecting the light that is scattered back to the detector. The light is typically delivered and detected with fiber-optic probes separated by a controlled distance ρ that has a direct effect on the interrogated tissue volume. To correct for the spectral profiles of the light source and detector, the measured backscattered intensity from the tissue is calibrated against that obtained from a material with known optical properties (known as a 'tissue phantom') [8]. This calibrated measurement, known as the diffuse reflectance $R_d(\lambda)$, can be directly related to $\mu_a(\lambda)$ and $\mu_s(\lambda)$ (and, consequently, to c_i, A, and b) using the diffusion approximation (DA) to the radiative transport equation. The DA is valid in regimes where the light has been scattered enough to be modeled as diffuse; this typically occurs when $\mu_s'/\mu_a > 10$. In non-diffuse regimes, such as locations close to the source and wavelengths where absorption from blood is very high (e.g. ~400–450 nm), the DA is no longer valid and Monte Carlo simulations are often employed to model light transport instead [9]. The flow of the DOS procedure, from data collection to calibration to mathematical modeling for extraction of tissue properties, is shown in Figure 1.

2.2. Diffuse optical tomography (DOT)

There are many different techniques for obtaining two-dimensional and three-dimensional maps of tissue properties using DOS measurements. These methods fall under the umbrella of DOT. One common DOT approach (Figure 2), which has been described by numerous groups [10–12], is to obtain diffuse reflectance at a number of different source–detector separations ρ and use a numerical inversion algorithm to obtain spatial maps of c_i, A, and b. These multi-fiber DOT probes have been widely employed *in vivo* for breast and brain imaging [10,13], but they

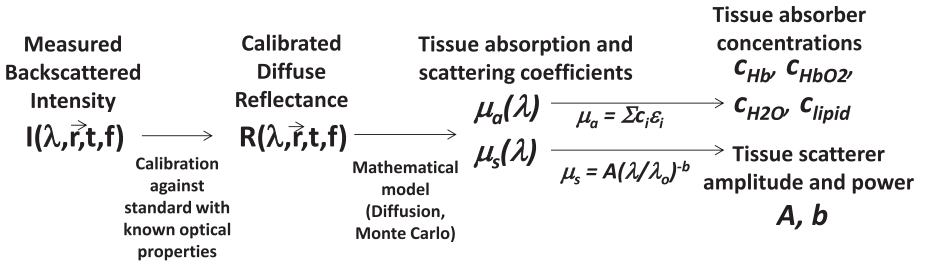

Figure 1. Flow of DOS method.

Notes: First, the measured backscattered intensity is obtained from the tissue sample and from a reference with known optical properties, enabling acquisition of the calibrated diffuse reflectance R_d of the tissue. Then, a mathematical model is employed to obtain the tissue absorption and scattering coefficients from the diffuse reflectance, and mathematical representations of $\mu_a(\lambda)$ and $\mu_s(\lambda)$ are employed to extract tissue absorber concentrations c_i, scattering amplitude A, and scattering power b.

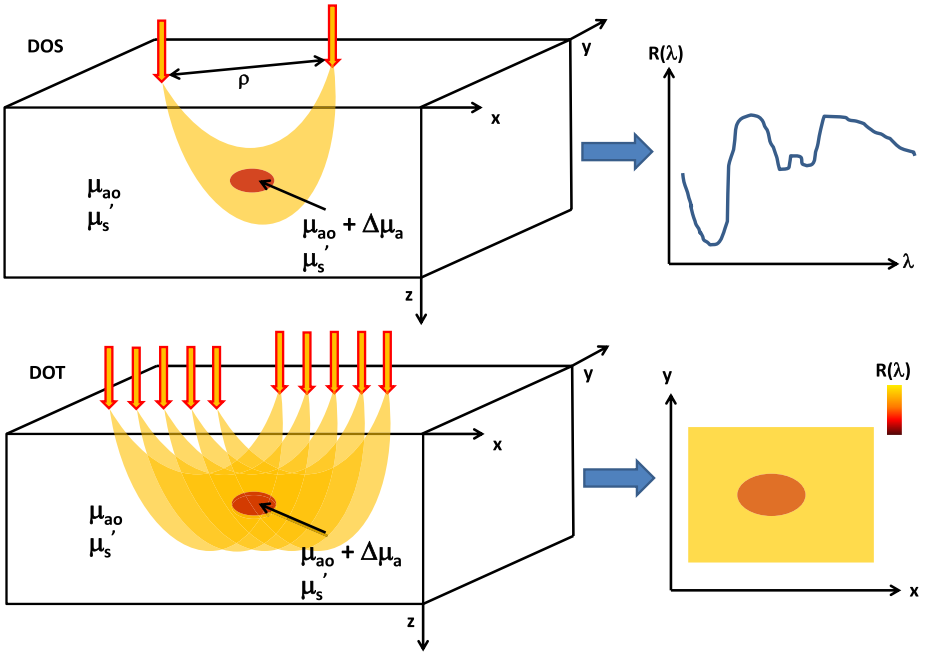

Figure 2. Schematics of common DOS (top) and DOT (bottom) measurement setups.

Notes: In DOS, light is delivered to the tissue via a source fiber and backscattered photons are detected via a detector fiber separated some distance ρ from the source. This source–detector separation plays a key role in controlling the region of tissue sampled by the majority of the photons. DOS measurements provide the reflectance at different wavelengths, enabling detection of spectral features of tissue absorption and scattering. In DOT, reflectance measurements at multiple source–detector pairs are employed to enable reconstruction of a two-dimensional map of the reflectance (and hence, absorption and scattering) at each wavelength.

typically suffer from low spatial resolution. Recently, wide-field DOT methods, in which a projected field of light is directed onto the sample and a camera detects the backscattered signal, have been employed for the reconstruction of optical properties with high (~1 mm) spatial resolution [14]. These methods typically

modulate the light at several different spatial frequencies in order to rigorously decouple the absorption and scattering coefficients [8].

In order to reconstruct three-dimensional maps of tissue optical properties, an additional set of measurements typically must be performed in order to provide depth sectioning of the interrogated tissue volume. This extra variable is often wavelength [15], time [16], or spatial (or temporal) frequency [17] of the incident light. Acquiring surface images of the tissue at different wavelengths can provide depth-sectioning capabilities because the tissue absorption and scattering properties are heavily wavelength-dependent, so the mean penetration depth of the photons can vary significantly with wavelength [15]. Time-gating of the detected photons also serves as a means to separate the photons that traveled different total path lengths (and thus, sampled different depths) within the tissue before returning to the surface [16].

2.3. Photoacoustic tomography (or microscopy) (PAT/PAM)

Photoacoustic techniques combine the penetration depth of ultrasound with the functional specificity of tissue optical absorption contrast to provide quantitative and high-resolution functional and structural maps of tissue deeper than 1 mm below the surface. Given that bulk of the reconstructive imaging in PAT and PAM rely on principles governing the propagation and detection of ultrasound waves in tissue and that intrinsic functional contrast in these techniques arises from the optically induced thermal pressure waves – something that is directly dependent on the optical absorption spectrum of tissue as discussed above – a full review of PAT/PAM techniques will not be provided in this review. However, we would like to emphasize that this area remains one of the most active areas of research in the realm of biomedical optics mainly because of the tremendous potential these methods for *in vivo* medical imaging, as discussed in several recent reviews [18–23].

2.4. Clinical applications of DOS and DOT: breast cancer

One common clinical application of DOS and DOT methods is the detection, characterization, and monitoring of breast cancer and its response to a variety of treatment mechanisms. Figure 3 shows maps of tissue absorber concentrations (oxygenated hemoglobin, ctO_2Hb; deoxygenated hemoglobin, ctHHb; water; lipid) of the right and left breast of a patient with cancer in the right breast [6]. The rightmost column is a map of a quantity known as the tissue optical index (TOI), defined by the equation TOI = $(ctH_2O/Lipid)(ctHHb)$ and determined empirically to be a combination of parameters that is particularly effective for highlighting contrast between tumors and surrounding normal tissue. The figure demonstrates the ability of DOS to reconstruct two-dimensional maps of tumor optical properties that correspond well to the spatial location and extent of the

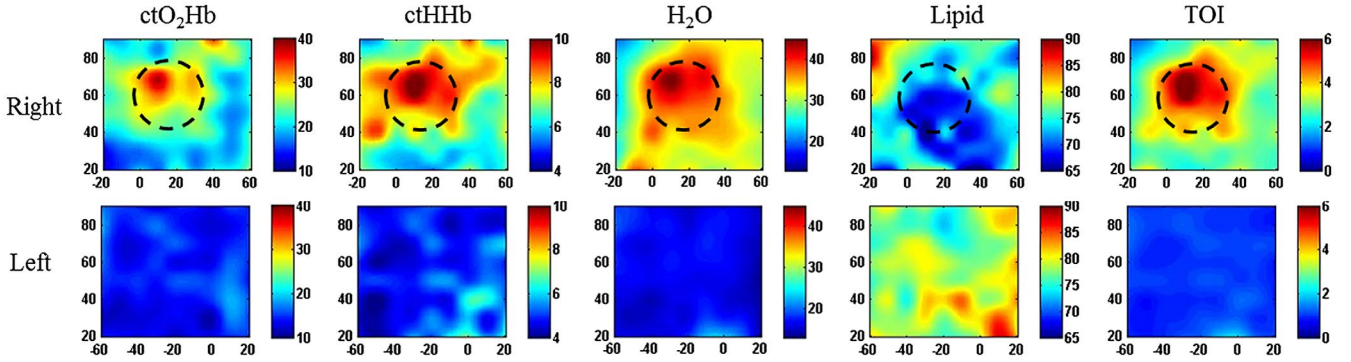

Figure 3. DOT maps of concentrations of oxygenated hemoglobin (ctO_2Hb), deoxygenated hemoglobin (ctHHb), water, and lipid in the breasts of a human subject with a cancerous tumor in the right breast.

Notes: The rightmost column is a map of the tissue optical index (TOI), defined by TOI = (ctH_2O/Lipid)(ctHHb). The changes in the measured optical parameters correspond well to the tumor region estimated by palpation (black-dashed circle) ([6], reproduced with permission).

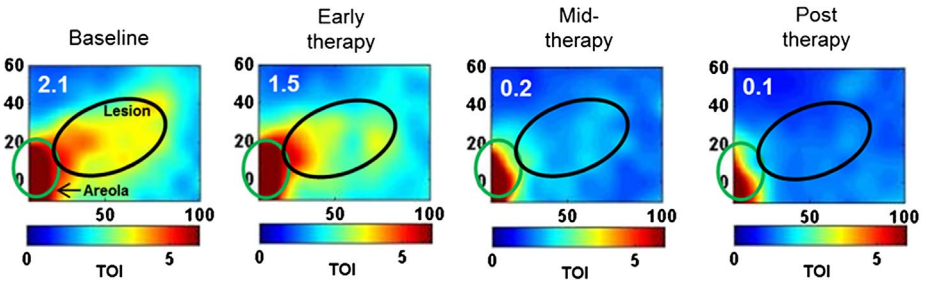

Figure 4. DOT maps of tissue optical index (TOI), defined by TOI = (ctH_2O/Lipid)(ctHHb), of the breast of a patient with a cancerous lesion (black elliptical region) at different time points throughout the process of neoadjuvant chemotherapy ([6], reproduced with permission).
Notes: The areola (green elliptical region) is used as a fiducial marker. The TOI maps demonstrate the successful treatment of the patient, who exhibited a pathologic complete response to the chemotherapy.

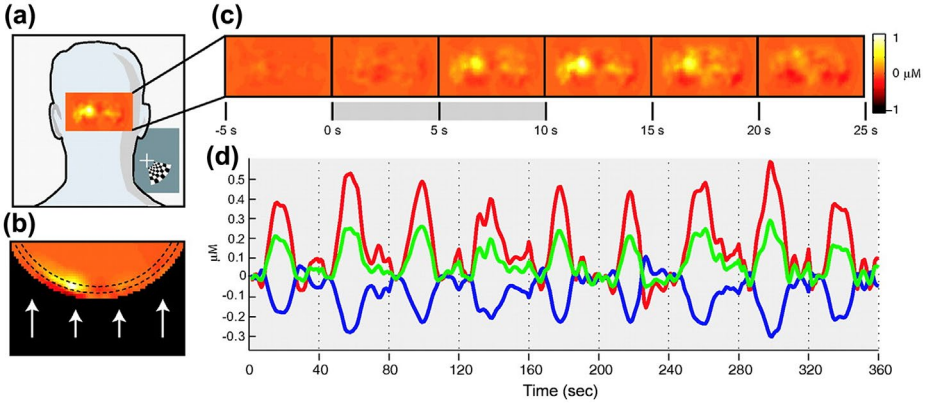

Figure 5. *In vivo* diffuse optical measurement of functional activation of the human brain using a DOS setup (left) with multiple sources (red) and detectors (blue) placed on the back of the head.
Notes: The DOS measurements provide spatial and temporal maps (a–c) of changes in hemoglobin concentration in the tissue in response to stimulus. Time courses (d) of changes in the concentrations of oxygenated hemoglobin (red), deoxygenated hemoglobin (blue), and total hemoglobin (green) can be calculated to characterize the brain's response to the stimulus ([24], reproduced with permission).

tumor (black-dashed circle), as determined by palpation. These methods have also been employed to monitor the response of breast tumors to neoadjuvant chemotherapy (Figure 4) and other types of treatment.

2.5. Clinical applications of DOS and DOT: functional brain imaging

DOS techniques have also been employed for functional brain imaging. Since DOS methods typically use near-infrared light, which can penetrate deep beneath the tissue surface, *in vivo* human brain imaging can be achieved using the appropriate combinations of wavelengths and probe source–detector separations [13]. One common DOS-based brain imaging experiment is the monitoring of the cerebral hemodynamic response to an external stimulus. Figure 5 shows the experimental

setup and results for such an experiment [24]. A probe containing a number of different sources and detectors is placed on the back of the head, enabling diffuse optical interrogation of the brain. As the brain responds to the stimulus, maps of changes in oxygenated hemoglobin concentration (Figure 5(c)) are reconstructed from the optical data. Time courses of changes in the concentrations of oxygenated hemoglobin, deoxygenated hemoglobin, and total hemoglobin (Figure 5(d)) can be calculated to characterize the hemodynamic response of the brain to the stimulus. This technique is of great potential use for quantitatively monitoring the brain's response to conditions such as stroke, traumatic brain injury, and Alzheimer's disease.

3. Coherence-based sensing approaches

As discussed in the previous section, diffuse optical imaging techniques rely on quantifying spatio-temporal changes of the detected light intensity by connecting them to differences in optical absorption or scattering properties of media, at one or more wavelengths. The phase of the electromagnetic optical fields is not considered to play any discernible role in these diffuse optical measurements. However, in interferometric detection, it is the phase differences between optical fields that are detected as intensity fluctuations. Interferometric sensing using coherent (laser) light sources is an extremely active area of research in field of translational biomedical optical imaging and we describe two important techniques – laser speckle contrast imaging (LSCI) and diffuse correlation spectroscopy (DCS) – that have been used in a number of clinical studies and are beginning to emerge as commercial options.

Before beginning the discussion about LSCI and DCS, we wish to state we will specifically not be discussing another important and widely used coherence-based optical imaging technique – optical coherence tomography or microscopy [25–28] (OCT/OCM) – here. This decision to focus primarily on non-OCT-based coherence-based optical tissue sensing stems from the fact that OCT is a very well-established clinical technique that has previously been extensively reviewed [29–38]. We also note that recent advances in Fourier and spectral domain Doppler OCT have been developed to enable functional sensing of blood flow velocities within intact tissues – also termed optical microangiography – and are well described elsewhere [39–42].

3.1. Laser speckle contrast imaging

The formation of laser speckle is a well-known phenomenon, especially given the ubiquity of coherent laser sources today. Laser speckle is mathematically described as a complex pattern resulting from the interference of a large number of coherent photon fields scattered off a rough object and therefore having random phases at the image plane [43]. Although the speckle pattern itself appears

chaotic and possess little semblance to any discernible features to the illuminated and imaged object, laser speckle has several quantifiable statistical features that can provide a wide range of information about spatio-temporal properties within the imaged scattering medium [44–47]. LSCI for biomedical imaging was demonstrated nearly four decades ago as an experimentally simple technique capable of non-invasively imaging microvascular flow in retinal tissues [48].

Experimental implementation of LSCI involves shining a coherent laser light source to uniformly illuminate a region of interest that is focused using a camera and involves collection of the raw speckle image with no ambient light [49,50]. Image analysis is performed to quantify blurring of the speckles recorded in the image by calculating a spatial contrast factor given by $K = \frac{\sigma}{\mu}$, where σ is the standard deviation and μ the mean of the intensity values recorded some set of pixels. These sets of pixels are usually selected as region of 7×7 neighbors in a square grid across all pixels in the acquired image as spatial averaging within a single acquisition, or across a series of images acquired as time series (or video data) [49]. Mathematically, the contrast factor can be shown to be related to the speed of the moving particles causing the blurring of the speckle pattern [46,51], which in biological tissues translates to a blood flow index. Although LSCI is experimentally simple to implement and has been shown to work even with low-cost laser diodes for sources and web cameras for detectors [52], there are several active and open areas of research including improving depth-sensitivity, developing improved theoretical models involved in the physics behind speckle formation, and in developing methods so that LSCI can generate quantitative blood flow maps [53–57].

3.2. Diffuse correlation spectroscopy

In DCS, optical fiber probes are used to launch a coherent source of light into the medium of interest and then measure intensity fluctuations across small areas (typically within diameters of 1–5 μm) several mm–cm from the incident source and at relatively high frequency (>1–5 MHz). The observed intensity fluctuations represent speckle intensity fluctuations caused due to motion of scattering particles moving through diffuse photon trajectories leading from the source–detector. The temporal autocorrelation of these speckle intensity fluctuations is the normalized intensity autocorrelation $g_2(\tau)$ and is related to the normalized field autocorrelation function $g_1(\tau)$ through the Siegert relationship: $g_2(\tau) = 1 + \beta(g_1(\tau))^2$ [58]. The normalized field autocorrelation $g_1(\tau) = G_1(\tau)/G_1(0)$, where $G_1(\tau)$ is related to the time-varying coherent electric field in the scattering and absorbing medium. $G_1(\tau)$ is modeled as propagating through the turbid media via a DOS-like diffusion equation but having an attenuating factor that depends both on the tissue absorption as well as the mean-squared displacement of a scattering particle – which is a function of the autocorrelation delay τ [59,60]. Thus, experimentally measured intensity autocorrelation $g_2(\tau)$ from DCS measurements, when supplemented with estimates of optical absorption and scattering properties at the laser wavelength

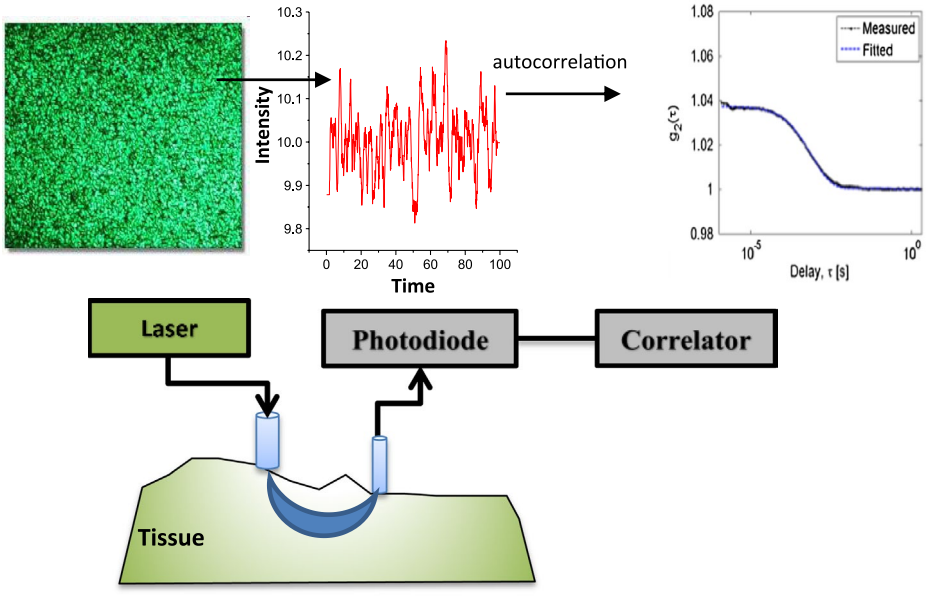

Figure 6. Illustration of DCS measurements in terms of speckle intensity fluctuations and experimental components required in measuring the autocorrelation trace.
Notes: It is critical in DCS to capture only a few speckles and thus the detection probe is usually 4–5 μm. The laser also needs to have a coherence length that is much longer than the mean photon path from the source to the detector.

(typically obtained from simultaneous or sequential DOS/DOT measurements), allow theoretical fitting of $g_2(\tau)$ using expressions for $G_1(\tau)$ [61,62].

Experimentally, Figure 6 illustrates the schematic relation between the incident laser speckle, the intensity fluctuations measured and its autocorrelation to the experimental components of typical DCS instrument. The choice of the laser coherence length (i.e. the maximum distance within the tissue for which the laser is expected to sufficiently maintain its coherent properties) must be such that it is much longer than the average path length of photons diffusing from the source and the detector placed on the tissue. Most researchers use laser sources with coherence lengths longer than 10 m. Detectors are small-area avalanche photodiodes running in photon counting mode whose digitized output is passed on to the autocorrelation device – usually a dedicated hardware board [61,62].

One burden with using DCS techniques has not only the need to have a long coherence length laser, but also to require autocorrelator boards for fast computation of the numerically intensive calculation of the autocorrelation function, which usually adds cost to the instrument. However, recent developments in theoretical analysis of the autocorrelation decays indicate the possibility that blood flow information may be acquired measuring the autocorrelation for few initial delay times [63].

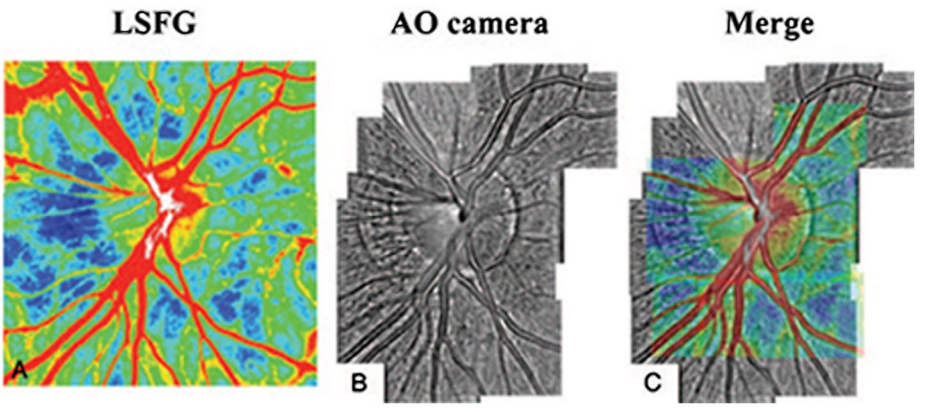

Figure 7. Representative merged figure from [72] (reproduced with permission). Laser speckle image (A) and adaptive optics image (B) were merged into (C).

3.3. Clinical applications of LSCI

Applications of LSCI have focused on using this technique to detect blood flow in tissue that are transparent (ocular blood flow [64,65]) or for tissue where the vasculature is more readily accessible from the surface (such as skin wound healing and open surgery [66–71]). Figure 7 below shows one particularly novel application of LSCI to differentially image arteries and veins in the human eye by superposing an adaptive optics image of the retinal bed with an LSCI image [72], it was shown that LSCI could be used to compute a retinal blood flow index to quantify. The color and contrast density of the merged image (Figure 7(C)) indicates mean blood flow rates for arteries in red and veins in gray.

3.4. Clinical applications of DCS

DCS has been more widely employed for a variety of clinical applications (relative to LSCI) for monitoring blood flow in the brain, skeletal muscle, bone, and during tumor growth [73–83]. Tissue blood flow changes measured using DCS have also been quantitatively matched to blood flow measured using ultrasound, MRI, and laser Doppler flow.

In the past, DCS instrumentation contained bulky electronic components and required significant logistical efforts for use in clinical settings. Recent efforts have focused on improving the form factor of these systems. One such application of DCS (Figure 8) provides a proof-of-principle example where employed a handheld DCS instrument (source–detector separation of 2.5 cm) to optically scan women with clinically confirmed malignant breast lesions as they were seated in the clinic in a supine position [84]. Measurements were acquired both on the ipsilateral breast – containing the malignant lesion – and on the contralateral normal tissue. DCS measurements were obtained in a line-scan by moving the device across

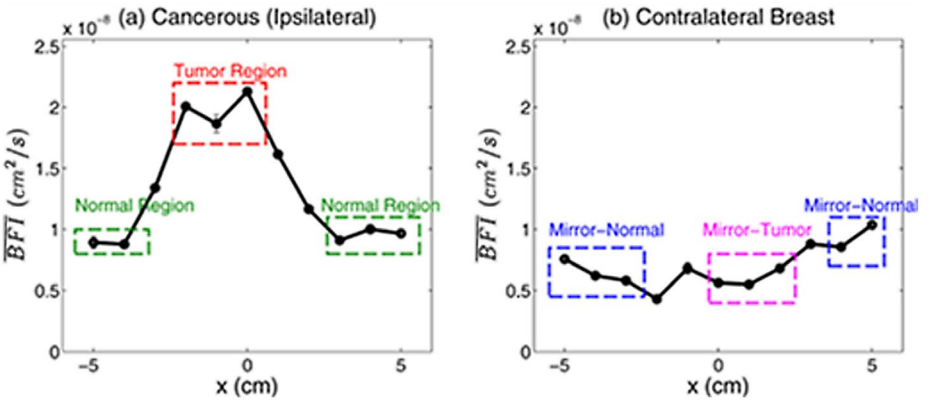

Figure 8. Line scans of BFI in (a) for ipsilateral cancerous breast and (b) for the normal contralateral breast, from [84] (reproduced with permission).
Notes: Locations of the (T) and normal (N) regions were chosen using radiological data to guide probe placement. Mirror locations of the tumor (MT) and normal (MN) regions (in the ipsilateral breast) are identified in the contralateral breast.

10 cm. Although these studies used a priori knowledge about the location of the tumors to make the DCS measurements, the extracted blood flow values (relative to the repeated errors) are more than double the value measure normal sites (on either breast). A diffuse correlation tomographic approach could be designed with multi-source–detector configurations to increase spatial sensitivities to yield a three-dimensional map of relative blood indices.

4. Nonlinear optical methods for label-free molecular sensing and imaging in living biological tissues

The theoretical principles and experimental techniques of nonlinear optics (NLO) are well known in physics and have been applied to numerous and diverse fields of study in the basic sciences and engineering [85]. In particular, a variety of NLO techniques have been applied to address fundamental and applied studies in biology and medicine [86–89], as illustrated in Figure 9, including exciting applications of two-photon excitation fluorescence (TPEF) and second-harmonic generation (SHG) to label-free molecular sensing and imaging in clinical medicine [90,91] and emerging *in vivo* applications of coherent anti-Stokes Raman scattering (CARS) [92].

Employing NLO techniques for medical applications presents some distinct advantages as well as challenges relative to approaches based on linear optics. For sensing and imaging applications in biological tissues, general advantages offered by NLO methods include the ability to interrogate specimens at greater tissue depths using longer (near-infrared, NIR) wavelengths that are subject to less optical loss from absorption and scattering, to optically section tissues and minimize out-of-focus photo damage while decreasing background, and to employ

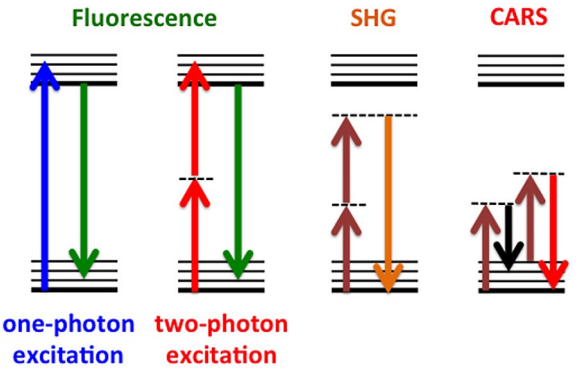

Figure 9. Schematic energy level diagrams for linear (one-photon excitation) fluorescence and nonlinear optical processes including two-photon excitation fluorescence (TPEF), second-harmonic generation (SHG), and coherent anti-Stokes Raman scattering (CARS).

label-free sensing with molecular specificity. In general, the greatest challenges to implementing NLO-based technologies clinically include high equipment costs, complexity of operation (both for data acquisition and analysis), and potential regulatory hurdles for human studies.

Here, we illustrate the utility of NLO methods for label-free molecular sensing and imaging in living biological tissues to address critical regulatory issues in tissue engineering and regenerative medicine (TE/RM). The fields of TE/RM have advanced to the point where tissues damaged by disease or trauma can be replaced with a living engineered tissue construct manufactured from the patient's own freshly harvested primary cells [93]. Generally, engineered tissue manufacturing processes take several days, are strictly controlled by regulatory agencies to ensure cell-based device effectiveness and patient safety, and require rigorous quality control testing on the day of product release to determine the most robust tissue construct to implant into the patient. One of the challenges facing the commercialization and clinical translation of TE/RM technologies is the unmet need for reliable, rapid quality control methods to assess construct viability without destroying or compromising the living, cell-based device and that yield quantified parameters employable as release criteria. Methods currently employed for the assessment of TE/RM products have serious limitations. For example, tissue histology is time-consuming and requires an invasive and destructive tissue biopsy, while biochemical assays of tissue culture media are non-invasive, but lack sensitivity by reporting parameters integrated over the entire construct without providing spatially localized information. An ideal quality control method would rapidly and non-invasively provide a quantitative, spatially localized assessment of tissue construct viability prior to product release and would be translatable to a clinical environment for *in vivo* assessment of the tissue construct post-implantation in patients.

Optical sensing methods based on endogenous tissue fluorescence have been suggested to characterize the structure and function of living, cell-based, tissue-engineered devices fabricated for implantation in clinical applications [94]. Rather than employing destructive cell viability assays or exogenous fluorescent dyes that are invasive to the cell manufacturing process, the label-free methods proposed target biologically and metabolically relevant endogenous cellular metabolic co-factors and extracellular structural proteins via NLO microscopic imaging techniques, including TPEF and SHG [95,96]. Endogenous fluorescent biomolecules that report on cellular metabolism and oxygen consumption include nicotinamide adenine dinucleotide (phosphate) (NAD(P)H) and flavin adenine dinucleotide (FAD), whose concentrations are related to cellular glucose uptake and energy consumption and production in metabolic pathways. Fluorescence lifetime imaging (FLIM) provides further information about the protein-binding states of cellular coenzymes [96]. Optical signals from endogenous structural proteins including keratin, elastin, and collagen report on the morphology and composition of the extracellular matrix, with SHG providing an excellent means for revealing collagen in biological tissues.

An illustration of using an NLO-based approach to characterize morphology and biochemistry in living engineered tissues is shown in Figure 10 [91]. While histological assessment would destroy the tissue construct, NLO microscopic imaging could be performed non-invasively via optical sectioning in three dimensions in the living tissue (left) under environmentally controlled and sterile conditions. Three-dimensional spatially localized information about cellular metabolic function, cellular spatial organization, and tissue microenvironment could be extracted from the optical data-sets via quantitative image analysis algorithms applied to cross-sectional (middle) and *en-face* (right) images. For example, the tissue's layered structure was visible in the destructive histology section (left) as well as the optically cross-sectioned image of endogenous cellular TPEF (NAD(P)H, cyan) with overlaid scaffold SHG (collagen, blue) (middle). Cellular viability information, primarily contained within TPEF signals from metabolic co-factors NAD(P)H and FAD, was obtained by optically sectioning thin cellular layers and using SHG signals to correct for extracellular matrix components (right). The acquired optical signals enabled tissue viability assessment via metrics of cellular spatial organization and metabolic function.

For these studies, cells and tissues were cultured from distinct primary human patient donors to intentionally introduce the intra-patient variability anticipated in clinical use [91]. Additionally, realistic stressing conditions anticipated during the biofabrication process were introduced to intentionally compromise cell viability. These experimental design features were introduced to challenge the reliability and robustness of the NLO approach, which successfully differentiated control from stressed constructs. This study was the first report demonstrating the ability of label-free NLO microscopy to characterize the viability of living cell-based devices manufactured with primary human cells. Thus, label-free NLO

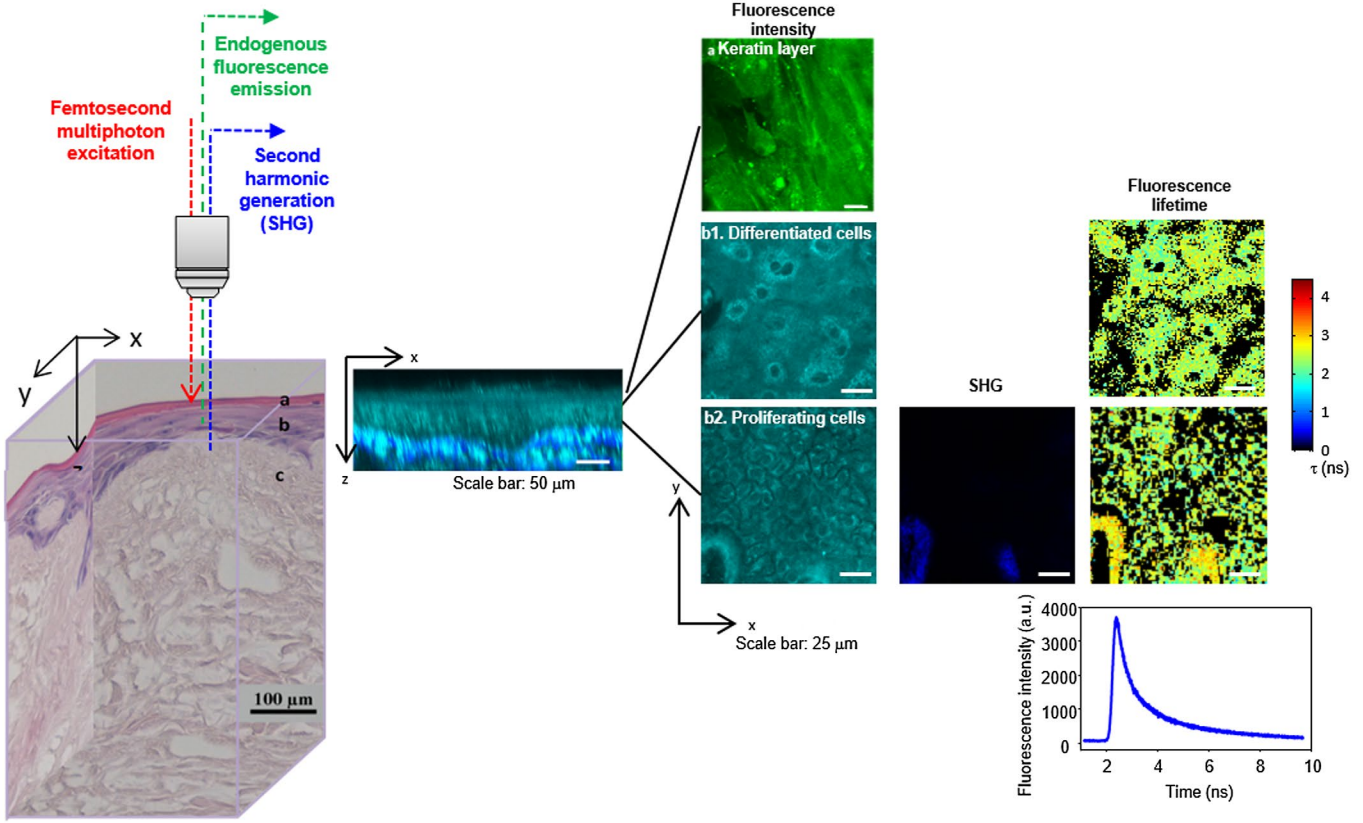

Figure 10. NLO imaging can be employed for non-invasive, label-free assessment of cell viability in living tissue engineered constructs prior to surgical implantation in patients to repair damaged tissues.

Notes: The living tissue construct (illustrated by the histology cube at left) is imaged microscopically via NLO techniques in three dimensions, generating both cross-sectional (middle) and *en-face* (right) images. Two-photon excited fluorescence (TPEF) microscopy, fluorescence lifetime imaging microscopy (FLIM), and second-harmonic generation (SHG) microscopic images are analyzed via quantitative algorithms to assess local tissue viability, including cellular metabolic function, spatial organization, and cellular microenvironment. (Figure reprinted from [91] with permission).

microscopic imaging was found to non-destructively provide reliable and quantitative release criteria for engineered human cell devices.

Thus, the microscopic detection of TPEF, FLIM, and SHG from endogenous constituents in living engineered tissue constructs provides information-rich multidimensional optical datasets that can be analyzed quantitatively to extract parameters linked to pre-implantation construct structure and function and, hence, the likelihood of *in vivo* graft success. In contrast to existing methods, these NLO-based methods for quality control enable rapid, quantitative, non-destructive, label-free, and spatially resolved assessment of engineered tissue construct morphology and viability. Thus, such NLO-based measures could serve as the basis for reliable manufacturing release criteria for cell-based tissue-engineered constructs prior to human implantation, thereby addressing a critical regulatory need in regenerative medicine.

5. Summary, perspectives, and conclusions

In this review, we have presented several key capabilities of diffuse, coherent, and nonlinear optical techniques for characterization of living human tissues. These methods provide quantitative, non- and minimally invasive means of assessing tissue structure and function, through physical parameters such as tissue absorber and scatterer concentrations, velocity of blood flow, and fluorescence from intracellular and extracellular tissue components.

The techniques discussed in this paper are able to probe a wide range of spatial and temporal scales. DOS/DOT and LSCI/DCS can provide sub-mm spatial resolution for quantifying optical properties on the so-called 'mesoscopic' length scale (between microscopic and macroscopic). Certain versions of these techniques can also be performed very rapidly, at upward of 50 Hz, to obtain information about pulsatile hemodynamics in living tissue [97]. Some DOS/DOT techniques, such as those involving streak cameras, can even enable near-ps scale temporal resolution to measure photon time-of-flight distributions in tissue [98,99]. NLO methods provide microscopic spatial resolution for imaging of structures such as cells and collagen fibers *in vivo* [91]. Certain NLO techniques, such as those involving fluorescence lifetime, can also provide sub-ns temporal resolution to quantify the dynamic behavior of fluorescent molecules in living tissue [91].

In terms of depth sectioning within tissue, DOS/DOT, LSCI/DCS, and NLO techniques are all typically associated with somewhat different spatial scales in the z-dimension. Diffuse methods such as DOS/DOT and DCS typically penetrate on the order of cm into the tissue, although the penetration depth is a strong function of probe source–detector separation and wavelength of incident light. Indeed, DOT methods typically employ a large number of different source–detector separations to enable depth-sectioning of several cm of tissue. By contrast, LSCI and NLO methods primarily interrogate the first few hundred microns to

1 mm beneath the tissue. NLO techniques are capable of sectioning with a high spatial resolution (dz ~ 10 microns) along the *z*-axis, suitable for separating the fluorescence of the superficial keratinized layer from that of the cellular layers in skin or a tissue-engineered construct (Figure 10). LSCI is not typically employed for depth-sectioning, although LSCI technology has been employed to characterize the penetration depth of photons in turbid media [100].

One major trend in tissue optics over the past decade has been the development of spectroscopy and imaging methods that combine multiple modalities to provide a more complete characterization of living tissue. An example of such a technique is the combination of diffuse optical methods (DOS/DOT) with coherence-based methods (LSCI/DCS) to provide information about tissue blood flow and oxygenation in tandem [101]. These combined flow/oxygenation technologies have the potential to help decouple flow-based hemodynamic parameters (e.g. reperfusion following injury or ischemia) from metabolism-based hemodynamic parameters (e.g. rate of oxygen consumption by tissue) [101]. When these types of multi-modal measurements are coupled with advances in imaging speed to acquire data at a rapid frame rate (e.g. >50 Hz) [97], the pulsatile nature of these hemodynamic parameters can also be characterized, providing information about vascular reactivity and compliance. These rapid, multi-modal imaging systems may enable the empirical development of more comprehensive models of the response of living tissue to different perturbations, providing a valuable inroad to understanding how the body responds to, and recovers from, trauma and disease.

Here, we have presented a review of several optical technologies (DOS/DOT, LSCI/DCS, and NLO methods) that are frequently employed for quantitative characterization of living biological tissue. Since these techniques rely on endogenous contrast arising from the subsurface tissue constituents, they are label-free and cause minimal perturbation to the structures being investigated. The quantitative nature of these technologies lends itself well to the development of standardized, objective, optical parameter-based metrics for tissue classification. Recent progression toward devices with smaller form factors and greater ease of use has facilitated gradual translation of biomedical photonic technologies into the clinic, paving the way for optical techniques to provide valuable assistance for a variety of tissue diagnostic and monitoring applications.

Disclosure statement

No potential conflict of interest was reported by the authors.

Funding

This work was supported in part by U.S. National Institutes of Health [1 TL1 TR 1415-1], [R44 DE021935-02].

References

[1] J.Q. Brown, K. Vishwanath, G.M. Palmer and N. Ramanujam, Curr. Opin. Biotechnol. 20 (2009) p.119.
[2] S.C. Kanick, C.v.d. Leest, R.S. Djamin, A.M. Janssens, H.C. Hoogsteden, H.J.C.M. Sterenborg, A. Amelink and J.G.J.V. Aerts, J. Thorac. Oncol. 5 (2010) p.981.
[3] W.R. Lloyd, R.H. Wilson, S.Y. Lee, M. Chandra, B. McKenna, D. Simeone, J. Scheiman and M.-A. Mycek, Biomed. Opt. Express 5 (2014) p.9.
[4] G. Zonios, L.T. Perelman, V. Backman, R. Manoharan, M. Fitzmaurice, J.V. Dam and M.S. Feld, Appl. Opt. 38 (1999) p.6628.
[5] I. Georgakoudi, B.C. Jacobson, J.V. Dam, V. Backman, M.B. Wallace, M.G. Müller, Q. Zhang, K. Badizadegan, D. Sun, G.A. Thomas, L.T. Perelman and M.S. Feld, Gastroenterology 120 (2001) p.1620.
[6] T.D. O'Sullivan, A.E. Cerussi, D.J. Cuccia and B.J. Tromberg, J. Biomed. Opt. 17 (2012) p.071311.
[7] S.L. Jacques, Phys. Med. Biol. 58 (2013) p.R37.
[8] D.J. Cuccia, F. Bevilacqua, A.J. Durkin, F.R. Ayers and B.J. Tromberg, J. Biomed. Opt. 14 (2009) p.024012.
[9] R.H. Wilson and M.-A. Mycek, Technol. Cancer Res. Treat. 10 (2011) p.121.
[10] R. Choe, A. Corlu, K. Lee, T. Durduran, S.D. Konecky, M. Grosicka-Koptyra, S.R. Arridge, B.J. Czerniecki, D.L. Fraker, A. DeMichele, B. Chance, M.A. Rosen and A.G. Yodh, Med. Phys. 32 (2004) p.1128.
[11] Z.-M. Wang, G.Y. Panasyuk, V.A. Markel and J.C. Schotland, Opt. Lett. 30 (2005) p.3338.
[12] D.A. Boas, D.H. Brooks, E.L. Miller, C.A. DiMarzio, M. Kilmer, R.J. Gaudette and Q. Zhang, IEEE Signal Process. Mag. 18 (2001) p.57.
[13] A.T. Eggebrecht, S.L. Ferradal, A. Robichaux-Viehoever, M.S. Hassanpour, H. Dehghani, A.Z. Snyder, T. Hershey and J.P. Culver, Nature Photon. 8 (2014) p.448.
[14] A. Mazhar, S. Dell, D.J. Cuccia, S. Gioux, A.J. Durkin, J.V. Frangioni and B.J. Tromberg, J. Biomed. Opt. 15 (2010) p.061716.
[15] S.D. Konecky, R.H. Wilson, N. Hagen, A. Mazhar, T.S. Tkaczyk, R.D. Frostig and B.J. Tromberg, Neurophotonics 2 (2015) p.045003.
[16] J. Chen, V. Venugopal and X. Intes, Biomed. Opt. Express 2 (2011) p.871.
[17] S.D. Konecky, A. Mazhar, D. Cuccia, A.J. Durkin, J.C. Schotland and B.J. Tromberg, Opt. Express 17 (2009) p.14780.
[18] V. Ntziachristos, Nat. Methods 7 (2010) p.603.
[19] J. Yao and L.V. Wang, Contrast Media Mol. Imaging 6 (2011) p.332.
[20] L.V. Wang and S. Hu, Science 335 (2012) p.1458.
[21] J. Allen and K. Howell, Physiol. Meas. 35 (2014) p.R91.
[22] L.V. Wang and L. Gao, Annu. Rev. Biomed. Eng. 16 (2014) p.155.
[23] A. Taruttis, G.M. van Dam and V. Ntziachristos, Cancer Res. 75 (2015) p.1548.
[24] B.W. Zeff, B.R. White, H. Dehghani, B.L. Schlaggar and J.P. Culver, Proc. Natl. Acad. Sci. USA 104 (2007) p.12169.
[25] J.M. Schmitt, IEEE J. Sel. Top. Quant. Electron. 5 (1999) p.1205.
[26] W. Drexler, M. Liu, A. Kumar, T. Kamali, A. Unterhuber and R.A. Leitgeb, J. Biomed. Opt. 19 (2014) p.071412.
[27] J.S. Schiffman, N.B. Patel, R.A. Cruz and R.A. Tang, Neuroimaging Clin. N. Am. 25 (2015) p.367.
[28] J. Kim, W. Brown, J.R. Maher, H. Levinson and A. Wax, Phys. Med. Biol. 60 (2015) p.R211.
[29] J. Welzel, Skin Res. Technol. 7 (2001) p.1.

[30] J. Chen and L. Lee, Clin. Exp. Optom. 90 (2007) p.317.
[31] D. Stifter, Appl. Phys. B-Lasers Opt. 88 (2007) p.337.
[32] A. Pizurica, L. Jovanov, B. Huysmans, V. Zlokolica, P. De Keyser, F. Dhaenens and W. Philips, Curr. Med. Imaging Rev. 4 (2008) p.270.
[33] J.L.B. Ramos, Y. Li and D. Huang, Clin. Exp. Ophthalmology 37 (2009) p.81.
[34] A. Petzold, J.F. de Boer, S. Schippling, P. Vermersch, R. Kardon, A. Green, P.A. Calabresi and C. Polman, Lancet Neurol. 9 (2010) p.921.
[35] J.J. Wong, T.C. Chen, L.Q. Shen and L.R. Pasquale, Semin. Ophthalmol. 27 (2012) p.160.
[36] C. Zivelonghi, M. Ghione, K. Kilickesmez, R.E. Loureiro, N. Foin, A. Lindsay, R. de Silva, F. Ribichini, C. Vassanelli and C. Di Mario, J. Cardiovas. Med. 15 (2014) p.543.
[37] D. Kohli, T.U. Shah and A.M. Zfass, Am. J. Gastroenterol. 110 (2015) p.S702.
[38] E. Jorge, R. Baptista, J. Calisto, H. Faria, P. Monteiro, M. Pan and M. Pêgo, J. Cardiol. 67 (2016) p.6.
[39] R. Agrawal, W. Xin, P.A. Keane, J. Chhablani and A. Agarwal, Expert Rev. Med. Devices 13 (2016) p.519.
[40] M.S. Mahmud, D.W. Cadotte, B. Vuong, C. Sun, T.W. Luk, A. Mariampillai and V.X. Yang, J. Biomed. Opt. 18 (2013) p.050901.
[41] R. Reif and R.K. Wang, Quant. Imaging Med. Surg. 2 (2012) p.207.
[42] R.K. Wang, IEEE J. Sel. Top. Quantum Electron. 16 (2010) p.545.
[43] J.W. Goodman, J. Opt. Soc. Am. 66 (1976) p.1145.
[44] M. Harris, Contemp. Physic. 36 (1995) p.215.
[45] D.D. Duncan, S.J. Kirkpatrick and R.K. Wang, J. Opt. Soc. Am. A 25 (2008) p.9.
[46] D. Briers, D.D. Duncan, E. Hirst, S.J. Kirkpatrick, M. Larsson, W. Steenbergen, T. Stromberg and O.B. Thompson, J. Biomed. Opt. 18 (2013) p.066018.
[47] D.D. Duncan, S.J. Kirkpatrick, J.C. Gladish and S.A. Hurst, Dyn. Fluctuations Biomed. Photonics Vi 7176 (2009) p.717603.
[48] A.F. Fercher and J.D. Briers, Opt. Commun. 37 (1981) p.326.
[49] D.A. Boas and A.K. Dunn, J. Biomed. Opt. 15 (2010) p.011109.
[50] A. Ponticorvo and A.K. Dunn, J. Visual Exp. 45 (2010) p.e2004.
[51] S. Yuan, A. Devor, D.A. Boas and A.K. Dunn, Appl. Opt. 44 (2005) p.1823.
[52] L.M. Richards, S.M.S. Kazmi, J.L. Davis, K.E. Olin and A.K. Dunn, Biomed. Opt. Express 4 (2013) p.2269.
[53] M.A. Davis, S.M.S. Kazmi and A.K. Dunn, J. Biomed. Opt. 19 (2014) p.086001.
[54] D.D. Duncan and S.J. Kirkpatrick, J. Opt. Soc. Am. A 25 (2008) p.2088.
[55] S.M.S. Kazmi, L.M. Richards, C.J. Schrandt, M.A. Davis and A.K. Dunn, J. Cereb. Blood Flow Metab. 35 (2015) p.1076.
[56] A.B. Parthasarathy, E.L. Weber, L.M. Richards, D.J. Fox and A.K. Dunn, J. Biomed. Opt. 15 (2010) p.066030.
[57] A.J. Strong, E.L. Bezzina, P.B.J. Anderson, M.G. Boutelle, S.E. Hopwood and A.K. Dunn, J. Cerebr. Blood Flow Metab. 26 (2006) p.645.
[58] G. Yu, T. Durduran, C. Zhou, R. Cheng and A.G. Yodh, *Near-infrared diffuse correlation spectroscopy (DCS) for assessment of tissue blood flow*, in *Handbook of Biomedical Optics*, D.A. Boas, C. Pitris and N. Ramanujam eds., Taylor & Francis, Boca Raton, FL, 2011, p.195–216.
[59] D.A. Boas, L.E. Campbell and A.G. Yodh, Phys. Rev. Lett. 75 (1995) p.1855.
[60] D.A. Boas and A.G. Yodh, J. Opt. Soc. Am. A 14 (1997) p.192.
[61] E.M. Buckley, A.B. Parthasarathy, P.E. Grant, A.G. Yodh and M.A. Franceschini, Neurophotonics 1 (2014) p.011009.
[62] T. Durduran and A.G. Yodh, NeuroImage 85 (2014) p.51.

[63] W.B. Baker, A.B. Parthasarathy, D.R. Busch, R.C. Mesquita, J.H. Greenberg and A.G. Yodh, Biomed. Opt. Express 5 (2014) p.4053.
[64] N. Himori, H. Kunikata, Y. Shiga, K. Omodaka, K. Maruyama, H. Takahashi and T. Nakazawa, Graefes Arch. Clin. Exp. Ophthalmol. 254 (2016) p.333.
[65] H. Kunikata, N. Aizawa, M. Kudo, S. Mugikura, F. Nitta, R. Morimoto, Y. Iwakura, Y. Ono, F. Satoh, H. Takahashi, S. Ito, S. Takahashi and T. Nakazawa, PLoS One 10 (2015) p.e0117452.
[66] A. Della Rossa, A. D'Ascanio, S. Barsotti, C. Stagnaro and M. Mosca, Scand. J. Rheumatol. (2016) p.1.
[67] S. Eriksson, J. Nilsson, G. Lindell and C. Sturesson, Med Devices (Auckl) 7 (2014) p.257.
[68] M. Ideguchi, K. Kajiwara, K. Yoshikawa, H. Goto, K. Sugimoto, T. Inoue, S. Nomura and M. Suzuki, J. Neurosurg. (2016) p.1.
[69] L.M. Richards, E.L. Towle, D.J. Fox Jr. and A.K. Dunn, Neurophotonics 1 (2014) p.015006.
[70] M. Ringkamp, M. Wooten, B.S. Carson Sr., M. Lim, T. Hartke and M. Guarnieri, J. Neurosurg. 124 (2016) p.422.
[71] B. Ruaro, A. Sulli, V. Smith, S. Paolino, C. Pizzorni and M. Cutolo, Microvasc. Res. 101 (2015) p.82.
[72] T. Iwase, E. Ra, K. Yamamoto, H. Kaneko, Y. Ito and H. Terasaki, Medicine (Baltimore) 94 (2015) p.e1256.
[73] G. Yu, T.F. Floyd, T. Durduran, C. Zhou, J. Wang, J.A. Detre and A.G. Yodh, Opt. Express 15 (2007) p.1064.
[74] S.A. Carp, N. Roche-Labarbe, M.A. Franceschini, V.J. Srinivasan, S. Sakadžić and D.A. Boas, Biomed. Opt. Express 2 (2011) p.2047.
[75] Y. Lin, L. He, Y. Shang and G. Yu, J. Biomed. Opt. 17 (2012) p.010502.
[76] T. Li, Y. Lin, Y. Shang, L. He, C. Huang, M. Szabunio and G. Yu, Sci. Rep. 3 (2013) p.1358.
[77] Y. Shang, K. Gurley and G. Yu, Anat Physiol 3 (2013) p.128.
[78] K. Verdecchia, M. Diop, T.Y. Lee and K. St. Lawrence, J. Biomed. Opt. 18 (2013) p.027007.
[79] Y. Shang, T. Li, L. Chen, Y. Lin, M. Toborek and G. Yu, Appl. Phys. Lett. 104 (2014) p.193703.
[80] T. Binzoni and F. Martelli, Appl. Opt. 54 (2015) p.5320.
[81] E.M. Buckley, B.F. Miller, J.M. Golinski, H. Sadeghian, L.M. McAllister, M. Vangel, C. Ayata, W.P. Meehan III, M.A. Franceschini and M.J. Whalen, J. Cereb. Blood Flow Metab. 35 (2015) p.1995.
[82] S. Han, M.D. Hoffman, A.R. Proctor, J.B. Vella, E.A. Mannoh, N.E. Barber, H.J. Kim, K.W. Jung, D.S. Benoit and R. Choe, PLoS One 10 (2015) p.e0143891.
[83] Z. Li, W.B. Baker, A.B. Parthasarathy, T.S. Ko, D. Wang, S. Schenkel, T. Durduran, G. Li and A.G. Yodh, J. Biomed. Opt. 20 (2015) p.125005.
[84] R. Choe, M.E. Putt, P.M. Carlile, T. Durduran, J.M. Giammarco, D.R. Busch, K.W. Jung, B.J. Czerniecki, J. Tchou, M.D. Feldman, C. Mies, M.A. Rosen, M.D. Schnall, A. DeMichele and A.G. Yodh, PLoS ONE 9 (2014) p.e99683.
[85] K. Rottwit and P. Tidemand-Lichtenberg, *Nonlinear Optics: Principles and Applications* (Optical Sciences and Applications of Light), CRC Press, Boca Raton, FL, 2014.
[86] W.R. Zipfel, R.M. Williams and W.W. Webb, Nat. Biotechnol. 21 (2003) p.1369.
[87] C.L. Evans and X.S. Xie, Annu. Rev. Anal. Chem. 1 (2008) p.883.
[88] B.R. Masters and P.T.C. So, *Handbook of Biomedical Nonlinear Optical Microscopy*, Oxford University Press, New York, 2008.
[89] W. Min, C.W. Freudiger, S. Lu and X.S. Xie, Annu. Rev. Phys. Chem. 62 (2011) p.507.
[90] K. König, J. Biophoton. 1 (2008) p.13.
[91] L.-C. Chen and W.R. Lloyd, Biomaterials 35 (2014) p.6667.

[92] M. Weinigel, H.G. Breunig, M.E. Darvin, M. Klemp, J. Röwert-Huber, J. Lademann and K. König, Phys. Med. Biol. 60 (2015) p.6881.
[93] M.H. Lee, J.A. Arcidiacono, A.M. Bilek, J.J. Wille, C.A. Hamill, K.M. Wonnacott, M.A. Wells and S.S. Oh, Tissue Eng. Part B: Rev. 16 (2010) p.41.
[94] W. R. Lloyd, L.-C. Chen and M.-A. Mycek, *Fluorescence spectroscopy* in *Optical Techniques in Regenerative Medicine*, S.P. Morgan, F.R. Rose, S.J. Matcher, eds., Ch.7, CRC Press – Taylor & Francis Group, Boca Raton, FL, 2013, p.171.
[95] T. Chang, M.S. Zimmerley, K.P. Quinn, I. Lamarre-Jouenne, D.L. Kaplan, E. Beaurepaire and I. Georgakoudi, Biomaterials 34 (2013) p.8607.
[96] L.-C. Chen, W.R. Lloyd, C.-W. Chang, D. Sud and M.-A. Mycek, *Fluorescence lifetime imaging microscopy for quantitative biological imaging*, in *Methods in Cell Biology Digital Microscopy* 4th ed., G. Sluder and D.E. Wolf, eds., Elsevier, San Diego, CA, 2013, p.457–488.
[97] K.P. Nadeau, T.B. Rice, A.J. Durkin and B.J. Tromberg, J. Biomed. Opt. 20 (2015) p.116005.
[98] S. Andersson-Engels, R. Berg, A. Persson and S. Svanberg, Opt. Lett. 18 (1993) p.1697.
[99] C.V. Zint, W. Uhring, M. Torregrossa, B. Cunin and P. Poulet, Appl. Opt. 42 (2003) p.3313.
[100] I.S. Sidorov, S.V. Miridonov, E. Nippolainen and A.A. Kamshilin, Opt. Express 20 (2012) p.13692.
[101] N. Roche-Labarbe, A. Fenoglio, H. Radhakrishnan, M. Kocienski-Filip, S.A. Carp, J. Dubb, D.A. Boas, P.E. Grant and M.A. Franceschini, NeuroImage 85 (2014) p.279.